The Continuum of 3D to 4D Treatment Delivery

Omid Nohadani[1,2] and Thomas Bortfeld[1]

1) Massachusetts General Hospital and Harvard Medical School, Department of Radiation Oncology, 30 Fruit St, Boston, MA 02114, USA
2) School of Industrial Engineering, Purdue University, 315 N. Grant Street, West Lafayette, IN 47907, USA

Abstract

Treatment planning based on respiration-correlated ("4D") CT has become more common in recent years. Still, treatment delivery is typically 3D, i.e., a "one plan fits all" (motion phases) approach. 4D delivery in principle offers greater flexibility but also greater challenges, both computational and practical. We develop a computational framework to open up some of the 4D flexibility without going all the way to 4D delivery. We apply our method to lung cases. The key result is that even for very complicated cases it is not necessary to do full unconstrained 4D delivery. A quasi-static delivery with 5% variability of intensity maps seems to suffice.

Keywords

Optimization, IMRT, 4D planning, 4D delivery, robustness.

Introduction

The management of organ motion and "4D" treatment planning have been areas of active research in the past few years. For disease sites with substantial respiratory motion, such as lung treatments, respiration correlated ("4D") CT scanning is in routine clinical use at many centres. However, even with 4D CT scanning, treatment techniques are almost always 3D, i.e., one treatment plan is being designed to cover all breathing phases, or all instances of geometry. 4D optimization techniques, which yield different treatment plans for different breathing phases, i.e., not only 4D planning but also 4D delivery, have been developed [1,2]. However, 4D delivery has not yet been applied prospectively in the clinic. There are numerous technical as well as computational challenges with 4D delivery.

We are interested in exploring simplified 4D delivery techniques that still exhibit some of the dosimetric advantages of 4D delivery. To that end, we develop a computational framework and will present a couple of examples of retrospective application to clinical cases.

In the rest of the paper we will assume that the 4D CT scan represents the extent of the motion fully. We do consider variations of the *duration* of the different breathing phases, but not variations in the spatial location of the phases. The latter would have to be taken into account with margins or with robust optimization [3,4], or possibly with adaptive planning strategies, which are beyond the scope of this paper. In other words, we consider motion but only to a limited degree the uncertainties of the motion.

Material and methods

We basically use our previous approach for 4D optimization (termed type 4 optimization in [1]), which results in different intensity-modulated plans for different breathing phases. If the motion were of the rigid body type, we would get a "tracking" delivery [5]. In general, we get a more complicated plan in which the intensity maps from phase to phase are not only shifted but also deformed relative to each other. As in Ref. [1], we choose a quadratic objective function given by

$$E(x) = \sum_{n\in\nu} \frac{\alpha_n}{|V_n|} \sum_{i\in V_n} \left[D_i(x) - D^{\text{pres}}\right]_+^2$$

where the dose is calculated via

$$D_i(\mathbf{x}) = \sum_{p\in \text{Phases}} \sum_{j\in \text{PB}_i} d_{ij}^{\,p} x_j^p .$$

Note that x is a vector of beamlet intensities x_j which depends on the phase p i.e., $\mathbf{x} = ((x^1_1; \ldots ; x^1_j; \ldots ; x^1_{\text{PB}}); \ldots ; (x^p_1; \ldots ; x^p_j ; \ldots ; x^p_{\text{PB}}); \ldots ; (x^P_1 ; \ldots ; x^P_j ; \ldots ; x^P_{\text{PB}})$.

Note that ν denotes the set of all voxels, divided in volumes of interests V_n with the corresponding weights α_n. In our new approach, the constraint optimization problem is:

$$\min_x \quad E(x)$$

$$\text{subject to} \quad \frac{\left(x_j^p - x_j^{(p+1) \bmod P}\right)}{\max\left(x_j^p, x_j^{(p+1) \bmod P}\right)} \le \Gamma, \quad p = 1,2,\ldots,P$$

$$x_j \ge 0, \quad \forall j \in \text{PB}.$$

The new constraint introduces the variability of the intensity maps $\mathbf{x}^p$ between neighbouring phases p and p+1. The parameter Γ allows us to explore a continuum between 3D optimization (with $\Gamma = 0$) on the one side, and fully 4D optimization (with $\Gamma = \infty$) on the other. Note that $\Gamma = 0$ forces all intensity maps in all phases to be the same, i.e., a 3D plan.

Specific implementation

We have implemented this framework in C++ using object-oriented tools and in a fashion that enables us to compute the dose to an anatomic voxel and its gradient with respect to the beamlet intensities. Thus, we can conduct a gradient-based optimization, which is highly efficient and does not require the detailed knowledge of the uncertainty. This capability allows for an extension to other sources of errors within the same framework, as discussed by [5]. Moreover, during each gradient-descent step, we adjust the step size in order to satisfy the Constraint (5). Since the step size is diminishing over the course of the iteration, the convergence criteria still holds.

For the dose calculation, we include organ deformation, which constitute nonrigid motion. The dose cubes for each phase are registered to the end-of-exhale volumes, using deformable image registration. We employ a B-spline deformable registration method, as discussed by [6], which is based on the Insight Segmentation Registration Toolkit. We compute the deformation vector using B-spline interpolation from the deformation values of points located in a course grid, which was a 50 mm cube. An expert identified homologous points in the end of inhale phase as well as in the end-of-exhale phase.

To avoid interplay of possible dosimetric uncertainties with motion and in order to warrant for highest accuracy, we employ Monte Carlo dose calculation for 6 MeV beams, as implemented in 4D MC developed by [7]. This efficient and accurate code accounts for beam hardening and tongue-and-groove effect by using first Compton scatter in the MLC medium. We extend the method to allow photon transport through the jaws and MLC using multiple Compton scatter. To incorporate temporal changes in the leaf position relative to the moving tumor target, different incidences in time are combined based on the prescribed monitor units, in order to reduce small MU effects.

In this work, we employ MC to generate the PB dose distributions for all the beamlets used in the optimization procedure and for 6 breathing phases. Therefore, these MC generated PBs account correctly for not only heterogeneity effects in the lung region but also motion effects. We developed the broad beam approach to generate Monte Carlo pencil beams (MCPB). For each beam direction, the X and Y jaws are set such that the PTV is encompassed within the jaw opening plus a 1-2cm margin to account for MLC delivery restrictions, penumbra and lateral scatter effects of the edge MCPBs. The MLCs are also placed such as to generate an identical field size as the jaw opening, guaranteeing an identical jaw and MLC field size. We then break up the open field into adjacent PB fluence squares, where all the particles within each PB fluence area are sampled to produce a
MCPB dose.

Results and discussion

To measure the continuum of 3D to 4D, we compare constrained 4D optimized plans with $\Gamma = 0$, $\Gamma = 0.05$ and $\Gamma = \infty$ on a clinical lung cancer patient from Massachusetts General Hospital (MGH). The prescribed dose to CTV is 63 Gy. Figure 1 illustrates a dose volume histogram for the 3D to 4D continuum. The beamlet intensities for neighboring phases is constrained by $\Gamma = 0$, $\Gamma = 0.05$ or $\Gamma = \infty$.

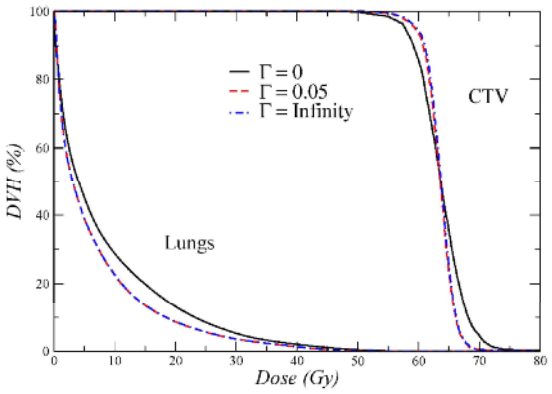

Figure 1 Dose-volume histogram: optimized IMRT plan base on Monte Carlo dose calculation when all six breathing phases are considered. The beamlet intensities for neighboring phases is constrained by $\Gamma = 0$, $\Gamma = 0.05$ or $\Gamma = \infty$.

Fig. 1 shows that the constraint $\Gamma=0$ performs sub-optimally compared with the other two solutions for $\Gamma>0$, and thus degrades the plan. However, it should be noted that with $\Gamma=0$ it was numerically difficult to find a solution because many steps of the iteration were infeasible, ie violating the constraints. More and longer optimization runs were therefore necessary. The

optimality cannot be guaranteed in this case. This difficulty can be avoided by defining the Γ=0 case as a separate 3D optimization problem, but this would be contrary to our objective to have one and the same method cover the whole spectrum from 3D to 4D optimization.
A relaxation of only 5% allows the 4D optimization method to find a plan that matches the prescribed objectives better. This improvement becomes only marginally better when we relax Γ completely at $\Gamma = \infty$. We also observe enhanced sparing of the lungs for any $\Gamma > 0$.

This observation is also apparent in the equivalent uniform dose (EUD). The EUD at $\Gamma = \infty$ is equal to 63.0 Gy, which in fact equates the prescribed dose. The EUD at $\Gamma = 0.05$ is 62.8 Gy which is only a 0.3% degradation. At $\Gamma = 0$, the EUD degrades down to 62.2, a reduction of 1.3%.

Fig. 2 illustrates the dose distribution for $\Gamma = 0.05$. It is apparent that most of the gain of employing all six phases can be achieved by slightly relaxing the constraint. The dose is very well conformed to the CTV.

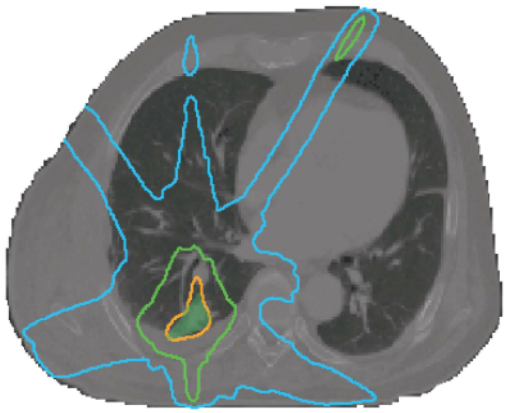

Figure 2 Dose distributions. The green shaded region marks the target. The contour lines are for 20%, 50%, 95%, and 105% of the prescribed dose. The 4D-optimized quasi-static ($\Gamma = 0.05$) plan, delivered to all phases.

Since the intensities of neighbouring phases are Γ – close to each other, it is expected that this plan will be robust against possible errors during treatment such as irregular breathing, i.e., when the breathing cycle is in a different phase than anticipated.

Conclusion

A framework to explore the continuum of 3D to 4D delivery, based on 4D planning, has been developed. Preliminary results indicate that a full 4D delivery implementation does not always provide a substantial advantage compared with quasi 3D delivery techniques, in which there is only a small or no dependence of the treatment delivery on the breathing phases. Future extensions of this work should identify those cases in which 4D delivery actually does have an advantage, and use simpler 3D delivery techniques for all other cases.

Acknowledgement

We are grateful to J. Seco for fruitful discussions on Monte Carlo dose calculations. This work was supported by the National Cancer Institute of the United States under grants R01-CA118200 and R01-CA103904.

References

[1] Trofimov A, Rietzel E, Lu H M, Martin B, Jiang S,Chen G T Y & Bortfeld T 2005 Phys. Med. Biol. **50** (12), 2779-2798.

[2] McQuaid D & Webb S 2008 Phys. Med. Biol. **53** (15), 4013-4029.

[3] Chu M, Zinchenko Y, Henderson S G & Sharpe M B 2005 Phys Med Biol **50** (23), 5463-5477.

[4] Chan 200 Chan T, Bortfeld T & Tsitsiklis J N 2006 Phys. Med. Biol. **51** (10), 2567-2583.6

[5] Martin B C, Bortfeld T R & Castanon D A 2007 Phys. Med. Biol. **52** (24), 7211-7228.

[6] Rueckert, D.; Sonoda L H C H D L M H D 1999 IEEE Transactions on Medical Imaging **18** (8), 712-721.

[7] Seco J, Sharp G, Wu Z, Gierga D, Buettner F & Paganetti H 2008 Med Phys **35**, 356-366.